Doppler Radiation Emitted by an Oscillating Dipole Moving inside a Photonic Band-Gap Crystal

Chiyan Luo, Mihai Ibanescu,* Evan J. Reed, Steven G. Johnson, and J. D. Joannopoulos

Department of Physics and Center for Materials Science and Engineering, Massachusetts Institute of Technology, Cambridge, Massachusetts 02139, USA

(Received 7 September 2005; published 2 February 2006)

We study the radiation emitted by an oscillating dipole moving with a constant velocity in a photonic crystal, and analyze the effects that arise in the presence of a photonic band gap. It is demonstrated through numerical simulations that the radiation strength may be enhanced or inhibited according to the photonic band structure, and anomalous effects in the sign and magnitude of the Doppler shifts are possible, both outside and inside the gap. We suggest that this effect could be used to identify the physical origin of the backward waves in recent metamaterials.

DOI: 10.1103/PhysRevLett.96.043903 PACS numbers: 42.70.Qs

The dispersion relations of photons can be drastically altered inside a photonic crystal [1–3], where strong, wavelength-scale-periodic dielectric modulations lead to absolute photonic band gaps (PBGs) [4]. This idea is the basis for many novel phenomena, including modified matter-light interaction [5–10] and unusual light refraction [11–14]. In particular, within a photonic crystal, a stationary oscillator with a frequency inside the PBG is forbidden to radiate. But what happens if the oscillator is moving with a constant velocity? In vacuum, the law describing the Doppler effect is elementary: the emission has a higher frequency value in the direction of the source's motion, and in the nonrelativistic limit the magnitude of the frequency shift is proportional to the source velocity. Doppler radiation was also studied long before in periodic waveguide systems, in the context of backward microwave oscillators [15] and cyclotron-resonance masers [16], and it was recognized that radiation can be generated at different frequencies separated by the spatial harmonic of the waveguide periodicity. Anomalous Doppler shifts have been found to occur when radiation reflects from shock waves propagating in photonic crystals and other periodic media [17–19].

Here, we analyze the Doppler effect within bulk photonic crystals and discuss, in particular, the effects due to the existence of a PBG. We use numerical simulations to study emission of Doppler radiation in photonic crystals, and show that radiation is emitted even when the source frequency lies within a band gap. Through comparison with the situation in vacuum, we show that the radiation amplitude can be enhanced or inhibited according to the photonic band structure, and that anomalous effects in the sign and magnitude of the Doppler shifts are possible, both outside and inside the gap. The reversed Doppler shifts we find are similar to those inside a left-handed material (LHM) [20], but can exist without a backward-wave effect. We suggest that the Doppler effect might be useful in understanding the origin of backward waves in the recent proposals of metamaterials capable of microwave negative refraction [21,22].

We consider a point source oscillating at frequency ω_0 and moving at velocity $\mathbf{v}$ inside a general photonic crystal. We take the current density $\mathbf{j}$ generated by this point source to be $\mathbf{j}(\mathbf{r}, t) = \mathbf{j}_0 e^{-i\omega_0 t}\delta(\mathbf{r} - \mathbf{v}t)$, neglecting relativistic time-dilation effects on ω_0. The current density can then be Fourier analyzed within unit total volume as $\mathbf{j} = \mathbf{j}_0 \sum_{\mathbf{k}} e^{i\mathbf{k}\cdot\mathbf{r} - i(\omega_0 + \mathbf{k}\cdot\mathbf{v})t}$, where the summation is over all wave vectors $\mathbf{k}$'s. The radiation can be found by summing up the response to each Fourier component of the source. Using the basis of Bloch waves, we obtain the electric field $\mathbf{E}$ as follows:

$$\mathbf{E}(\mathbf{r}, t) = \sum_{n,\boldsymbol{l},\mathbf{G}} \frac{4\pi i[\omega_0 + (\boldsymbol{l} + \mathbf{G})\cdot\mathbf{v}]\mathbf{j}_0 \cdot \mathbf{e}^*_{n,\boldsymbol{l},\mathbf{G}}}{\omega_n^2(\boldsymbol{l}) - [\omega_0 + (\boldsymbol{l} + \mathbf{G})\cdot\mathbf{v}]^2} \times \mathbf{E}_{n,\boldsymbol{l}} e^{-i[\omega_0 + (\boldsymbol{l}+\mathbf{G})\cdot\mathbf{v}]t}, \quad (1)$$

where the summation is over all band-index n's, all Bloch wave vector $\boldsymbol{l}$'s in the first Brillouin zone, and all reciprocal-lattice vector $\mathbf{G}$'s. $\omega_n(\boldsymbol{l})$ is the photon frequency in the nth band and at the Bloch wave vector $\boldsymbol{l}$. These Bloch waves have electric field distribution $\mathbf{E}_{n,\boldsymbol{l}} = \sum_{\mathbf{G}} \mathbf{e}_{n,\boldsymbol{l},\mathbf{G}} e^{i(\boldsymbol{l}+\mathbf{G})\cdot\mathbf{r}}$, normalized according to $\int d\mathbf{r}\boldsymbol{\epsilon}(\mathbf{r})\mathbf{E}^*_{n,\boldsymbol{l}} \cdot \mathbf{E}_{n',\boldsymbol{l}'} = \delta_{n,n'}\delta_{\boldsymbol{l},\boldsymbol{l}'}$. The poles of Eq. (1) give the resonantly excited photon frequencies $\omega_n(\boldsymbol{l})$ in the far field:

$$\omega_n(\boldsymbol{l}) = |\omega_0 + (\boldsymbol{l} + \mathbf{G})\cdot\mathbf{v}|. \quad (2)$$

Note that the expression inside the absolute-value sign in Eq. (2) can be negative. For each n, $\mathbf{G}$, and a given direction of $\boldsymbol{l}$, Eq. (2) gives a propagating Bloch wave. In addition, the direction of the average energy flow and thus the location in real space to observe the Bloch wave is determined by the group velocity $\partial\omega/\partial\boldsymbol{l}$ of that mode. Equation (2) can be intuitively understood by considering the crystal viewed from the reference frame of the moving dipole. The frequency $(\omega_0 + \boldsymbol{l}\cdot\mathbf{v})$ is the ordinary Doppler-shifted frequency that would occur for the dipole propagating through vacuum. However, because the dipole "sees" the crystal moving past it, it effectively sees an oscillating

potential with frequency $\mathbf{G} \cdot \mathbf{v}$ for each Fourier component $\mathbf{G}$ of the lattice. These frequency components of the potential mix with the ordinary Doppler-shifted frequency in order to emit photons of additional frequencies. It is interesting to note the mathematical similarity between Eq. (2) and the corresponding equation for the cyclotron-resonance maser interaction [16]: $\omega(\mathbf{k}) = \mathbf{k} \cdot \mathbf{v} + n\omega_c$, where ω_c is the cyclotron frequency $eB/\gamma m$ and n is an integer. The additional term in both equations is due to a periodicity of the interaction: the oscillation of the electron in the magnetic field for the cyclotron-resonance maser case and the oscillating dielectric ''potential'' for the case we study here.

We start our analysis with a one-dimensional (1D) nonrelativistic situation and consider, for example, the forward radiation seen by a far-field observer collinear with $\mathbf{v}$ (taken to be the z direction). We approximate the summation over l_z in Eq. (1) by a contour integral in the upper half plane, whose residues represent the far field. The radiation thus consists of all modes determined by Eq. (2), each excited with an amplitude $4\pi \mathbf{j}_0 \cdot \mathbf{e}^*_{n,l,\mathbf{G}} D$, in which we define

$$D = \frac{1}{|\frac{\partial \omega_n(l_z)}{\partial l_z} - v|} \tag{3}$$

to be the density of radiation states, which reduces to the usual density of states for 1D photonic crystals when $v = 0$. For nonzero v, D increases as the group velocity decreases toward v, and thus high radiation amplitudes can occur near the frequency where the group velocity vanishes, for example, near a PBG edge [23]. To obtain the specific radiation frequencies from Eq. (2), in Fig. 1 we plot the straight lines $\omega = |\omega_0 + (l_z + G_z)v|$, indexed by the different G_z's, on the band structure for all the photon modes propagating in the z direction $\omega = \omega_n(l_z)$. The intersections give all the radiation modes according to Eq. (2), and the slopes $\partial\omega_n/\partial l_z$ of the band structure at these intersections give the corresponding group velocities. Only those with $\partial\omega_n/\partial l_z > v$ travel ahead of the source and can be observed in the forward far field. Because the right-hand side of Eq. (2) can always fall within a propagating photonic band for a suitable $\mathbf{G}$, the Doppler radiation can always exist but may have a very small amplitude in some cases. We analyze several qualitatively different situations as follows: (i) When ω_0 lies within a photonic band, multiple frequencies are excited [Fig. 1(a)], corresponding to the multiple space harmonic ($\mathbf{G}$ component) of the Bloch eigenmodes with frequencies roughly $v\Delta G_z$ apart. For $v \ll c$, $D(\omega_n(l_z)) \approx D(\omega_0)$ and their amplitude is determined by $\mathbf{j}_0 \cdot \mathbf{e}^*_{n,l,\mathbf{G}}$. These results are similar to what has been known in waveguides with periodic modulations. By using a photonic crystal in which either $D(\omega_n(l_z))$ or $\mathbf{e}^*_{n,l,\mathbf{G}}$ is designed to be different from that in free space, the amplitudes of Doppler radiation can be

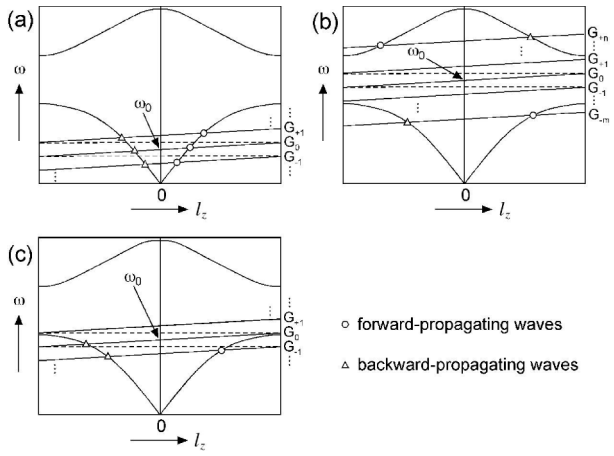

FIG. 1. Graphical construction of radiation frequencies of a moving source of frequency ω_0 in a photonic crystal. (a)–(c) The cases when ω_0 is within a band, inside a PBG, and near a band edge, respectively. The source waves are the straight lines, which are indexed by the reciprocal-lattice vectors $G_0 = 0$, G_{+1}, G_{-1}, etc., and whose intersections with the band structure give the radiation modes. The modes marked with circles are propagating along the $+z$ direction, and those marked with triangles are traveling opposite to the source.

enhanced or inhibited with respect to those in vacuum. Note that both positive and negative Doppler frequency shifts exist in general. (ii) When ω_0 lies within a forbidden band gap, the radiation of frequency ω_0 becomes evanescent waves and surrounds the source in a photon-atom bound state [5]. However, this bound state is now modulated by the periodic environment the source sees as it travels through the crystal, and radiation can be generated at the frequencies that fall within a propagating band by an addition or subtraction of the modulation harmonics. The source thus radiates at allowed band frequencies that is significantly different from ω_0 [Fig. 1(b)], giving an anomalous Doppler shift magnitude that is not proportional to v and is largely determined by the photonic band structure. Physically, this effect means that an excited atom with its transition frequency in a PBG moving in a photonic crystal can decay radiatively. (iii) Whereas both positive and negative frequency shifts occur in general with comparable strengths for ω_0 within a band, new features can occur for ω_0 near a band edge. The presence of a PBG forbids emission at frequencies inside the gap, and therefore for appropriate ω_0 the Doppler shifts can be all positive or all negative. Figure 1(c) shows such a situation where only negative shifts occur, and a moving source will radiate with a frequency *lower* than ω_0 in its forward direction. This effect is similar to but must not be confused with the reversed Doppler effect predicted in a LHM. The physical origin of the present effect is a complex Bragg scattering effect, i.e., the simultaneous action of periodicity and PBG, and is very different from that in a LHM, which is due to the simultaneously negative permittivity and

permeability. The present negative Doppler shift thus exists independent of backward-wave effects and can be expected in all bands, even those with forward-propagating waves ($\partial\omega/\partial l_z > 0$), as shown in Fig. 1(c). Now we apply the above analysis together with numerical simulations to the case of a two-dimensional (2D) square lattice of metallic rods in air, with lattice constant a and rod radii $r = 0.2a$. For simplicity, we model the metallic components as ideal metals and neglect any field or loss inside the rod region. The band structure of this photonic crystal is shown in Fig. 2, in which a plasmon PBG exists for $\omega \leq 0.5(2\pi c/a)$, and there is also a Bragg PBG around $\omega = 0.8(2\pi c/a)$. Using the finite-difference time-domain method, we perform numerical experiments of a source moving uniformly on an all-air path along the [10] direction in the middle of the neighboring rods through the crystal (the z axis). The source is chosen to be a continuous-wave dipole pointing along the rods' axis and oscillating at the frequency ω_0. Our computational cell is rectangular and in the xz plane, sufficiently long in the z direction ($>1000a$) so that reflections do not enter the results during the finite simulation time, and one lattice constant wide with periodic boundary conditions in the lateral x direction. Such an arrangement is experimentally interesting because it avoids direct collisions of the source with the crystal. It also guarantees that the far-field radiation away from the moving source consists of modes traveling along the z direction with $l_x = 0$, i.e., a quasi-1D situation along ΓX. We monitor the radiation on a point that has the same x coordinate with the source but is at least $10a$ away through the simulation, and obtain the frequency spectrum of the Doppler radiation by a direct Fourier transform in time.

The simulation results are shown in Fig. 3 for various ω_0's and a source velocity $v = 0.01c$, which corresponds to a 1% Doppler frequency shift in vacuum. The photonic-crystal and vacuum cases are shown on the same plot for comparison of the peak frequencies. From Fig. 3(a), it is clear that the moving source with a frequency in the plasmon PBG, $\omega_0 = 0.47(2\pi c/a)$, radiates at frequencies $\geq 0.51(2\pi c/a)$, which exhibits a Doppler shift more than 8 times larger than the shift in vacuum. In addition, the peak emission occurs near the bottom band edge of the crystal, a position almost independent of the source velocity, with an amplitude about $1/8$ of that in vacuum. This situation can thus be viewed as a Doppler effect with an anomalously large shift magnitude as described before. When ω_0 increases to $0.55(2\pi c/a)$, which is inside the first photonic band, the emission spectrum is shown in Fig. 3(b). Here several radiation peaks appear that are separated in frequency by roughly $0.01(2\pi c/a)$, and the dominant emission is about 4 times stronger than in the vacuum case. This effect can be explained by the slowdown of the radiation group velocity and the increased field strength along the path of the source in the photonic

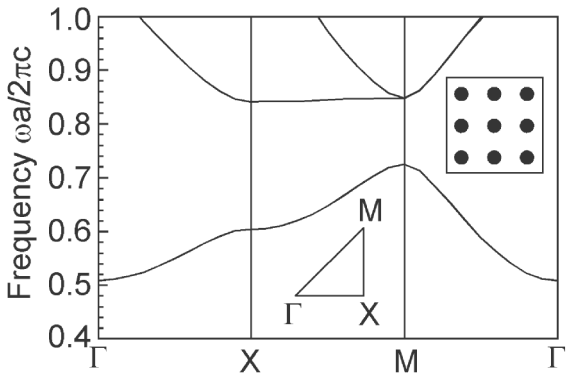

FIG. 2. Band structure of a 2D square lattice of metallic rods in air of lattice constant a. The insets show the irreducible Brillouin zone and a 3×3 block of the crystal (black filled circles stand for the metallic rods).

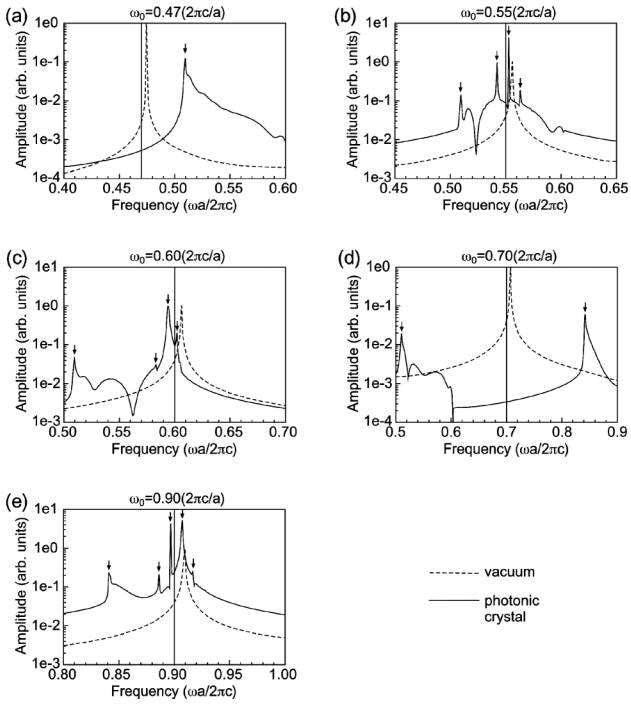

FIG. 3. Numerical simulation results of the Doppler effect shown on a logarithmic scale. The source velocity is $v = 0.01c$. (a)–(e) The frequency spectra of the radiation monitored in the far field ahead of the source, for ω_0 starting from $0.47(2\pi c/a)$ and ranging up to $0.90(2\pi c/a)$. The results for the photonic crystal shown in Fig. 2 are shown in the solid curves and those for vacuum are shown in the broken curves for comparison of peak frequencies. The various frequency peaks for the photonic-crystal radiation are indicated by arrows. Because of the finite simulation time, there is a smooth background signal, and not all frequencies are resolved. The value of ω_0 in each case is also noted in vertical lines. The peak amplitudes for emission in vacuum have been normalized to unity.

crystal. For $\omega = 0.60(2\pi c/a)$ [Fig. 3(c)], which is near the band edge, the radiation frequencies that correspond to positive Doppler shifts are suppressed to smaller amplitudes by the Bragg PBG, and the dominant emission peak occurs at a negatively Doppler-shifted frequency. The case of $\omega_0 = 0.70(2\pi c/a)$, which is inside a Bragg PBG, is shown in Fig. 3(d) and is qualitatively similar to that in Fig. 3(a). The Doppler shifts in this case are very large in magnitude and occur on either side of the PBG [24], with amplitudes inhibited to a level below 10% of that in vacuum. Finally, Fig. 3(e) shows the radiation spectrum for $\omega_0 = 0.90(2\pi c/a)$, which is in the second photonic band having a negative group velocity. Here there are two dominant emission peaks at $0.907(2\pi c/a)$ and $0.897(2\pi c/a)$, and the positive-shifted peak (the same sign as the vacuum Doppler shift) has a slightly stronger magnitude. This is consistent with our analysis and demonstrates that the electrodynamics associated with negative group velocity bands in photonic crystals is in general not equivalent to those in a LHM.

We speculate that the nonrelativistic Doppler effect could be employed to determine the physical origin of the negative refraction recently observed in wires or split-ring-resonator structures [21,22]. A dominant negative Doppler shift within a propagating band (not close to a band edge) can be produced only by a backward-wave effect in a uniform material and therefore validates the hypothesis of a negative index. On the other hand, if multiple emission frequencies with comparable amplitudes as in Fig. 3(c) occur, the metamaterials might simply be viewed as a photonic crystal, with negative refraction induced by backward waves due to complex Bragg scattering effects [13]. Results for Doppler radiation in the wires or split-ring-resonator structures therefore might be used as a clue to resolve recent controversies [25,26].

The flexibility of a photonic-crystal environment allows for new degrees of freedom in manipulating the Doppler radiation. For example, the amplitudes at the multiple emission frequencies may be enhanced or inhibited by judiciously designing the photonic lattice structure with the appropriate field profile, e.g., using a superlattice. While our discussion has focused on the Doppler interaction of point sources with a metallic photonic crystal, an entirely similar analysis can be extended to dielectric photonic crystals. These results should be immediately appropriate for experimental studies in the microwave regime, where powerful radiation sources such as cyclotron resonance in electron beams exist.

This work was supported in part by the Material Research Science and Engineering Center program of the National Science Foundation under Grant No. DMR-9400334 and the Department of Defense (Office of Naval Research) Multidisciplinary University Research Initiative program under Grant No. N00014-01-1-0803.

*Electronic address: michel@mit.edu

[1] E. Yablonovitch, Phys. Rev. Lett. **58**, 2059 (1987).
[2] S. John, Phys. Rev. Lett. **58**, 2486 (1987).
[3] J. D. Joannopoulos, R. D. Meade, and J. N. Winn, *Photonic Crystals: Molding the Flow of Light* (Princeton University Press, Princeton, NJ, 1995).
[4] K. M. Ho, C. T. Chan, and C. M. Soukoulis, Phys. Rev. Lett. **65**, 3152 (1990).
[5] S. John and J. Wang, Phys. Rev. Lett. **64**, 2418 (1990).
[6] Z. Y. Li, L. L. Lin, and Z. Q. Zhang, Phys. Rev. Lett. **84**, 4341 (2000).
[7] J. B. Pendry, A. J. Holden, W. J. Stewart, and I. Youngs, Phys. Rev. Lett. **76**, 4773 (1996).
[8] C. M. Cornelius and J. P. Dowling, Phys. Rev. A **59**, 4736 (1999).
[9] Z. Y. Li, Phys. Rev. B **66**, 241103 (2002).
[10] C. Luo, M. Ibanescu, S. G. Johnson, and J. D. Joannopoulos, Science **299**, 368 (2003).
[11] S.-Y. Lin, V. M. Hietala, L. Wang, and E. D. Jones, Opt. Lett. **21**, 1771 (1996).
[12] H. Kosaka, T. Kawashima, A. Tomita, M. Notomi, T. Tamamura, T. Sato, and S. Kawakami, Phys. Rev. B **58**, R10 096 (1998).
[13] M. Notomi, Phys. Rev. B **62**, 10 696 (2000).
[14] C. Luo, S. G. Johnson, J. D. Joannopoulos, and J. B. Pendry, Phys. Rev. B **65**, 201104(R) (2002).
[15] J. R. Pierce, *Traveling-Wave Tubes* (Van Nostrand, New York, 1950).
[16] J. L. Hirshfield and V. L. Granatstein, IEEE Trans. Microw. Theory Tech. **25**, 522 (1977), and references therein.
[17] E. J. Reed, M. Soljacic, and J. D. Joannopoulos, Phys. Rev. Lett. **90**, 203904 (2003).
[18] E. J. Reed, M. Soljacic, and J. D. Joannopoulos, Phys. Rev. Lett. **91**, 133901 (2003).
[19] N. Seddon and T. Bearpark, Science **302**, 1537 (2003).
[20] V. G. Veselago, Sov. Phys. Usp. **10**, 509 (1968).
[21] D. R. Smith, W. J. Padilla, D. C. View, S. C. Nemat-Nasser, and S. Schultz, Phys. Rev. Lett. **84**, 4184 (2000).
[22] R. A. Shelby, D. R. Smith, and S. Schultz, Science **292**, 77 (2001).
[23] The mode with $\partial\omega_n/\partial l_z = v$ travels at the source velocity and represents the near-field waves beyond our approximation.
[24] Our simulations also show that the frequencies near the upper edge of the first band, $0.6(2\pi c/a)$, are not efficiently excited, a result beyond our simple 1D model.
[25] A. L. Pokrovsky and A. L. Efros, Phys. Rev. Lett. **89**, 093901 (2002).
[26] R. Marques, J. Martel, F. Mesa, and F. Medina, Phys. Rev. Lett. **89**, 183901 (2002).